Template Matching of Freeform Surfaces Based on Orthogonal Distance Fitting for Precision Metrology

Xiangqian Jiang[1], **Xiangchao Zhang**[1], **Paul J Scott**[1,2]

[1] Centre for Precision Technologies,University of Huddersfield, HD1 3DH, UK
[2] Taylor-Hobson Ltd, PO Box 36, 2 New Star Road, Leicester, LE4 9JQ, UK

E-mail: x.jiang@hud.ac.uk

Abstract. Freeform surfaces are widely used in advanced optical and mechanical devices. In order to assess the form quality of a freeform surface, it is required to match the measurement surface with the design template. To improve the matching efficiency and accuracy, the whole procedure is divided into two stages, rough matching and final fitting. A new rough matching method, called the structured region signature is proposed. The structured region signature is a generalized global feature which represents the surface shape by a one dimensional function. The template location occupying the best matching signature is considered to be the correct rough position of the measurement surface. After that the motion parameters are updated iteratively based on the orthogonal distance fitting. The dependency between the foot-point parameters of the projection points and the motion parameters is derived from the closest-distance relationship between correspondance point pairs. Numerical experiments are given to demonstrate the validity of this approach.

PACS numbers: 06.20.Dk, 06.60.Sx, 07.05.Tp

Keywords: freeform surface, form error evaluation, matching, orthogonal distance fitting Submitted to: *Meas. Sci. Technol.*

1. Introduction

Traditionally, most industrial components are composed of simple geometries like planes, spheres and cylinders. With the development of science and technologies, more and more particular functions are required on the components, for example, an F-theta lens is used to provide a flat image field at the plane of interest in laser printers, and the airplane wings and fuselage is required to reduce the aerodynamic resistance. The simple shaped components do not meet these requirements. Therefore more and more new essential components with *freeform surfaces* (also termed *sculptured surfaces* or *curved surfaces* [1]) are being developed by researchers and manufactured by industry. In metrology, freeform surfaces are defined as the surfaces which have no invariance degree [2], i.e. a freeform surface has no symmetry in translation or rotation.

The surface form plays an essential role in the characteristics of freeform components. The form error of simple geometries is assessed by terms of flatness, roundness, sphericity etc involving gauges for different shapes and applications [3]. For complex-shaped surfaces, e.g. marine propellers [4], it requires highly skilled technicians to check the surface with numerous mechanical gauges. In optical engineering, the form qualities of optics are generally tested with the Newton or Fizeau interferometer [5]. A quality test plate or a reference surface is required. The inspection in this way depends heavily on the technician's proficiency and the manufacturing accuracy of the test plates or gauges. It is evident that the task is very inefficient and expensive; more importantly, the inspection accuracy cannot be guaranteed. Consequently various automatic techniques have been developed– a design template is provided as a reference to represent the nominal shape of a freeform component and discrete data are measured from the component by instruments. The deviation between the measurement data and the template is regarded as the form error of the freeform surface and can be calculated quantitatively with mathematical techniques. In this way human operation is no longer necessary, thereby greatly saving time and cost, at the same time, improving the evaluation accuracy.

Usually the measured data are not exactly located in the same coordinate system with the template, and the form error cannot be obtained by directly subtracting the reference template from the data. Slight misalignment between the two coordinate systems can cause serious errors in the evaluation of the form quality. This is fatal for some key freeform elements which have higher form accuracy and perform critical functionality. Misalignment shall be eliminated to bring the template and data into a common coordinate system.

Matching (also referred to as *localization*, *alignment* [6], *registration* or *best-fitting*) is generally formulated as an optimization problem involving the search for motion parameters (three rotation angles and a translation vector) that minimize an objective function which quantifies the matching quality, such as the average squared distance between the two surfaces,

$$E = \sum_{i=1}^{N} \|\mathbf{q}_i - (\mathbf{R}\mathbf{p}_i + \mathbf{t})\|^2 \tag{1}$$

where $\mathbf{q}_i$ is the correspondance template point of an arbitrary measurement point $\mathbf{p}_i$. $\mathbf{R}$ is the optimal rotation matrix and $\mathbf{t}$ is the translation vector.

At present, there is a lack of practical and effective methods to characterize the form qualities of freeform surfaces. This paper presents an effective algorithm to match smooth freeform surfaces for precision coordinate metrology.

2. Review of Related Work

The most straightforward way to match the measurement data with the nominal surface is to minimize the objective function in Equation (1) using derivative-based algorithms. However, the convergence domains of these methods are very small and a good initial guess is required, otherwise false matching solutions can be yielded. Consequently various techniques have been developed to supply a rough matching between surfaces in different fields, e.g. computer aided design, computer vision and pattern recognition etc.

Some researchers utilize simple features on the surfaces. Wang et al [7] employed feature points, feature lines, and feature planes. The gravity centre is defined to be the feature point and the best fitted plane is taken as the feature plane. The feature line is defined as the vector from the gravity centre pointing to the farthest point on the surface. Then the two surfaces can be aligned based on these features. Cheung et al [8] proposed a five-point method. Five characteristic points are defined for each surface respectively–the gravity centre and four corner points. Then the gravity centres are overlapped and the measurement surface is rotated to minimize the sum of the distances between the five characteristic point pairs. These two methods suppose that the template and the measurement surface are of the same size and approximately from the same location. But usually the measured data is only one small region of the design template, hence global features like gravity centre or normal vectors will be invalid.

If the the measured surface includes some salient features like holes, slots, pockets etc, these features can be adopted to align the model and the measurement data [9, 10]. However, most smooth freeform surfaces do not contain any salient features, thus these methods are not very suitable in such cases. Some mathematical features, like moments, invariances, Fourier descriptors, correlations etc are globally defined on the entire surface or in the overlapping area for computer vision and image processing [11, 12, 13]. These methods are not sufficiently representative for geometric details. Some local features, like curvatures, shape index, integral volume descriptor etc can also be adopted as shape descriptors [14, 15, 16]. These methods establish correspondances between points or point groups by comparing the descriptor values and distance constraints. Transformation between the two surfaces is calculated with a clustering/voting method. Because these descriptors are usually calculated from a point and its neighbourhood using derivative methods, they are very sensitive to measurement noise and outliers, thus are prone to false matching results. In the computer vision field, some generalized features (also termed *shape descriptors* or *signatures* [17]) are defined, such as the spin image [18], point signature [19], geometric histogram [20] etc. They usually break down the 3D information of the surface into a stack of 2D descriptors on which robust 2D image matching techniques can be applied. These methods are effective and robust to match smooth freeform surfaces. However, it is very computationally expensive to extract and compare these locally defined generalized features.

When a rough position is supplied by the initial matching, refinement is carried out thereafter to obtain higher matching accuracy. The ICP (*Iterative Closest Point*) algorithm is the most popular final optimization method [21, 22]. This method establishes correspondance pairs between the measurement data and the template points, and iteratively calculates the optimal transformation parameters to minimize the distances between the correspondance pairs. This method can register

several types of geometric data such as point sets, triangle sets, implicit surfaces or parametric surfaces, and has no particular restrictions on the surface shape. It is very computationally expensive to establish point correspondances. The iterative process tends to be trapped at a local minimum [23], because of the non-convex character of the optimization task. Therefore many variations have been developed for the ICP method to improve the efficiency and accuracy [24].

If a continuous representation of the nominal template is supplied or the template is easy to reconstruct from discrete point sets, derivative based methods, such as the Gauss-Newton, steepest gradient descent and Levenberg-Marquardt algorithms can be adopted [25]. Many researchers paid attention on the fitting of simple geometries like quadric surfaces [26, 27, 28, 29], but the fitting methods of freeform surfaces have not been well developed. Fitzgibbon fitted 3D complex surfaces using the Levenberg-Marquardt algorithm by minimising the Huber estimator in the z direction[30]. Boggs et al proposed an algorithm to minimize the mean squared orthogonal distance for explicit complex surfaces [31]. Sourlier [32] discussed the fitting of parametric surfaces based on orthogonal distance regression. For each measured point $\mathbf{p}_i$, the foot-point parameters $\mathbf{u}_i$ associated with the correspondance point $\mathbf{q}_i$ were required to indicate its location on the nominal surface. The dependency between the motion parameters and the foot-point parameters of the correspondance points were ignored. This will reduce the accuracy of the fitted results.

3. The Structured Region Signature Method

Unlike traditional industrial components and simple geometries, most smooth freeform surfaces do not have any salient features or shape parameters to be utilized for matching and alignment. Based on Chua et al's point signature [19], this paper proposes a novel generalized feature, called the *Structured Region Signature* (SRS) to describe the shape of freeform shapes.

3.1. Definition of the Structured Region Signature

Given a freeform surface consisting of discrete points, $\mathbf{P} = \{\mathbf{p}_i \in \mathbb{R}^{3\times 1}, i = 1, 2, \cdots, N\}$, the central point $\mathbf{c} = [x_c, y_c, z_c]^T$ on the surface is selected and a sphere is constructed centred at $\mathbf{c}$ with a radius R such that it is cut into two parts by the surface. To make the signature more descriptive, the radius R should be as large as possible provided that the sphere is within the boundary of the surface. Practically, R is selected to be the smallest distance from $\mathbf{c}$ to the boundary, as shown in Figure 1(a). All the points lying within the sphere (they are called *region points* and denoted with dots in Figure 1(b)) constitute a region *Re*. A plane $\mathbf{p}$ is fitted through the region, i.e. a plane $ax + by + cz + e = 0$ such that,

$$(a, b, c, e) = \arg\min \sum_{\mathbf{p}_i \in Re} \frac{(ax_i + by_i + cz_i + e)^2}{a^2 + b^2 + c^2} \tag{2}$$

where $\mathbf{p}_i = [x_i, y_i, z_i]^T$ is an arbitrary region point.

In practice, the normal vector $\mathbf{n} = [a, b, c]^T$ of the plane is calculated with an eigenvector method. Firstly a 3×3 symmetric covariance matrix is constructed,

$$\mathbf{A} = \sum_{\mathbf{p}_i \in Re} (\mathbf{p}_i - \mathbf{p}_c)(\mathbf{p}_i - \mathbf{p}_c)^T \tag{3}$$

where $\mathbf{p}_c$ is the gravity centre of all the region points.

If $\lambda_1 \geq \lambda_2 \geq \lambda_3$ denote the eigenvalues of $\mathbf{A}$ associated with unit eigenvectors $\mathbf{v}_1, \mathbf{v}_2$ and $\mathbf{v}_3$ respectively, $\mathbf{v}_3$ [33] is taken to be the normal vector $\mathbf{n}$.

A new plane $\mathbf{p}'$ is defined by moving the best-fitted plane $\mathbf{p}$ to go through the centre point $\mathbf{c}$, without changing the normal vector $\mathbf{n}$. The function of the new plane $\mathbf{p}'$ is,

$$a(x - x_c) + b(y - y_c) + c(z - z_c) = 0$$

or rewritten as

$$ax + by + cz + e' = 0 \tag{4}$$

Then an appropriate number, e.g. N_c of region points lying nearest to the sphere surface are selected to constitute a circle, see Figure 1(b). These circle points are projected onto the plane $\mathbf{p}'$ and the signed projection distances are,

$$d_i = ax_i + by_i + cz_i + e', i = 1, 2, \ldots, N_c \tag{5}$$

The corresponding projection points $\{\mathbf{p}'_i\}$ on the plane are

$$\begin{bmatrix} x'_i \\ y'_i \\ z'_i \end{bmatrix} = \begin{bmatrix} x_i - ad_i \\ y_i - bd_i \\ z_i - cd_i \end{bmatrix} \tag{6}$$

To make the surface signature independent of the orientation and position of the surface, a local cylindrical coordinate system is defined, by setting the signature centre $\mathbf{c}$ as the original point and defining the normal vector as the z axis $[0, 0, 1]^T$, thus yielding the projection plane $\mathbf{p}'$ to be the r–θ plane. Hence the signed distances $\{d_i\}$ of all the circle points form a one dimensional function with respect to the azimuth angles $\{\theta_i | -\pi < \theta_i \leq \pi, i = 1, 2, \cdots, N_c\}$, as shown in Figure 1(d). This distance profile is called the SRS of the surface.

3.2. The Matching Procedure using the SRS Method

The measurement surface is usually only one small region of the design template, thus the real correspondance location of the measurement surface is unknown on the template. The core idea of this initial matching method is to construct SRSs $\{St_i | i = 1, 2, \ldots, N_s\}$ on some selected plausible correspondance locations on the template using the same radius R with the measurement signature Sm. The location which occupies the most similar signature with that of the measurement surface is regarded to be the best matching. The matching procedure is illustrated in Figure 2.

If the surface is smooth, the signature curve should also be smooth. However, the circle points are not exactly located on the sphere. This will introduce undulations on the signature curve, causing the SRS not to faithfully describe the surface shape. Therefore all the signature profiles are interpolated with some smoothing techniques, e.g. least squares cubic splines [34].

As the two coordinate systems of the measurement surface and the template are probably misaligned, there may be a relative shift ϕ in the azimuth angle between their signature profiles. Given a template signature St_i and the measurement signature Sm, the similarity between them is evaluated with *the structure function*,

$$\{St_0, \phi_0\} = \arg\min \int_{-\pi}^{\pi} [Sm(\theta + \phi) - St_i(\theta)]^2 \, \mathrm{d}\theta \tag{7}$$

where $-\pi < \phi \leq \pi$ is the azimuth shift between the two signatures.

Practically, the signature curves are sampled uniformly with an appropriate interval, e.g. $2\pi/N_c$. Thus the signature curves become discrete date set $\{S(\theta_k)|k = 1, 2, \cdots, N_c\}$ and the candidate shift angles will be,

$$\phi_j = \frac{\pi}{N_c}(2j - N_c), j = 1, 2, \cdots, N_c$$

Subsequently Equation (7) will have a discrete representation,

$$\{St_0, \phi_0\} = \arg\min \sum_{k=1}^{N_c} \left[Sm(\theta_k + \phi_j) - St_i(\theta_k)\right]^2 \tag{8}$$

After all the signatures are compared, the location associated with the signature St_0 and shift angle ϕ_0 which occupies the least dissimilarity value is regarded as the best matching. Here the centre of the measurement signature is denoted with $\mathbf{c}_m$, the centre of the best-matching template signature St_0 is $\mathbf{c}_t$, and the two corresponding normal vectors are $\mathbf{n}_m$ and $\mathbf{n}_t$ respectively.

The measurement surface is rotated thereafter to align the two normal vectors. Three unit vectors are defined to construct two orthonormal frames for measurement and template surfaces,

$$\begin{cases} \mathbf{n}_0 = (\mathbf{n}_m \times \mathbf{n}_t)/\|\mathbf{n}_m \times \mathbf{n}_t\| \\ \mathbf{n}_1 = (\mathbf{n}_m \times \mathbf{n}_0)/\|\mathbf{n}_m \times \mathbf{n}_0\| \\ \mathbf{n}_2 = (\mathbf{n}_t \times \mathbf{n}_0)/\|\mathbf{n}_t \times \mathbf{n}_0\| \end{cases} \tag{9}$$

Then the rotation matrix to align the two orthonormal frames is,

$$\mathbf{R}_1 = [\mathbf{n}_t, \mathbf{n}_0, \mathbf{n}_2] \times [\mathbf{n}_m, \mathbf{n}_0, \mathbf{n}_1]^T \tag{10}$$

Because there is a shift angle ϕ_0 between the two signatures, the measurement surface needs to be rotated about the normal vector $\mathbf{n}_t = [a_t, b_t, c_t]^T$. This rotation matrix is [36],

$$\mathbf{R}_2 = \begin{bmatrix} c + n_x^2(1-c) & n_z s + n_x n_y(1-c) & -n_y s + n_x n_z(1-c) \\ -n_z s + n_x n_y(1-c) & c + n_y^2(1-c) & n_x s + n_y n_z(1-c) \\ n_y s + n_x n_z(1-c) & -n_x s + n_y n_z(1-c) & c + n_z^2(1-c) \end{bmatrix}$$

where $s = \sin(\phi_0)$ and $c = \cos(\phi_0)$.

Finally the measurement surface is translated to overlap the two signature centres, and the new measurement surface is,

$$\mathbf{P}' = \mathbf{R}_2\mathbf{R}_1(\mathbf{P} - \mathbf{c}_m) + \mathbf{c}_t \tag{11}$$

3.3. Implementation Issues

If the discrete points are very sparse on the surface, the circle points will not be located sufficiently close to the sphere surface, which will cause unnecessary undulations on the signature curve. In fact, the most exact way to obtain a signature curve is not to interpolate the discrete circle points, but directly to calculate the intersection curve between the freeform surface and the sphere. However it is usually very computationally expensive. In this case, a new circle can be obtained by moving the circle points iteratively toward the sphere surface,

$$\begin{cases} x_i \leftarrow x_i + (1 - \|\mathbf{p}_i\mathbf{c}\|/R)(x_i - x_c) \\ y_i \leftarrow y_i + (1 - \|\mathbf{p}_i\mathbf{c}\|/R)(y_i - y_c) \\ z_i \leftarrow f(x_i, y_i) \end{cases} \tag{12}$$

In the equation, $\mathbf{p}_i = [x_i, y_i, z_i]^T$ is an arbitrary circle point, $\mathbf{c} = [x_c, y_c, z_c]^T$ is the signature centre, R is the radius of the signature sphere and $z = f(x, y)$ is the analytical function of the freeform surface. If the template is given as a parametric function, this can be interpolated by solving a nolinear point-inversion problem[35]. It is demonstrated that usually via several iterations, the circle points will be very close to the sphere surface and a smooth signature curve can be obtained. To make the signature more descriptive, more points can be sampled on one signature circle, and multiple concentric circles can be employed for one signature. Consequently the signature can represent the shape in several bounding areas and more geometrical information can be involved.

The template signature centres are discrete points sampled on the template. It is almost impossible to find the exact correspondance location of the measurement surface. The goal of the SRS matching is to find the candidate location which is nearest to the real correspondance position. If the rough correspondance area is already known before matching, it is feasible to arrange signature centres with a higher density at this area. At the template area where the surface shape changes greatly, signatures can have significant difference even at two locations that are very near to each other. Therefore, the candidate locations will be sampled with their density proportional to the surface curvatures. If no prior knowledge is supplied about the rough correspondance location or the surface is very smooth, the template signature centres can be sampled uniformly with an appropriate spacing. It is apparent that if a higher density is adopted, the matching error can be reduced. But more signatures need to be calculated and compared, which will subsequently increase the computational expense. To solve this problem, the template signature centres can be selected in a coarse-to-fine approach, i.e. first sampling centres with a bigger spacing, and then sampling centres with a smaller spacing around the neighbourhood of the current best-matching location. This is repeated until the matching result is good enough or the spacing is sufficiently small.

The SRS matching method is based on the assumption that the template location whose signature is the most similar with the measurement signature is nearest to the real correspondance location. But this may not necessarily be true. The signature curve is taken from the circle points and only the surface shape at this bounding area is involved, rather than the shape of the whole surface, and hence there may be many locations having nearly the same signature curve, especially for the surfaces which include symmetric parts. As a result of measurement noise and calculation error, the location occupying the best-matching signature may be an incorrect one. That is to say, the real correspondance location will have a well matched signature, but the signature which is the most similar to the measurement signature may not be at the correct correspondance location. To solve this problem, a residual-checking strategy is employed. All the plausible matching locations are sorted in an ascending order by their signature structured functions in Equation (8). The matching residual of each location is checked successively. Once the preset residual threshold is satisfied, the checking process is terminated and a correct location is found. Here, the RMSE (Root Mean Squared Error) of the residual is adopted as a metric to assess the matching quality.

3.4. Utilization of SRS

The spin image method [18] is a very popular representation for image registration. It creates a local 2D image for each chosen oriented point. For each neighbourhood point, only the distances to the fitted plane and to the normal vector are recorded and the azimuth angle are ignored. At least two spin images are needed to restrict 6 degrees of freedom in the 3D space, subsequently the involved region of each image will be much smaller than the measured surface. Since the surface shapes used in precision engineering are normally very smooth and local shape variations are not so remarkable, as a consequence not much geometrical information can be included in each image. That means the spin image method may lead to false correpondances. On the contrary, SRS utilizes all the heights and azimuth angles along the entire circle of each signature, instead of accumulating them together. Thus only one SRS is sufficient to establish the relative matching between two surfaces.

Compared with Chua and Jarvis' point signature [19], SRS does not need to calculate intersection curves between the freeform surface and the placed spheres, hence the computational cost is greatly reduced. More importantly, the point signature method decides the rotation angle ϕ about the normal vector by overlapping the two points which have the greatest projection distances. When the surface is nearly symmetric, there may be several points which have similar projection distances, consequently false matching will be caused. However SRS records all the angular locations sampled from each signature and decides the azimuth angle by minimising the difference between the two signature curves. Therefore it can make the best use of the shape information in the signature curves and a more reliable matching result can be obtained. Furthermore, the point signature is locally defined at a small area on the surface whilst SRS is a global one. Since most freeform surfaces in the precision metrology field are very smooth, there will not be significant difference between the locally defined signatures. Therefore the point signature is not appropriate for application in precision engineering either.

It is worth noting that SRS does not work well for non-smooth surfaces. It is based on the assumption that two locations near to each other have similar signatures. This holds true for most smooth freeforms surfaces. If a surface contains great shape variation, sharp edges, peaks, pits or steps, the signatures will be significantly different even when the two locations are very near to each other. Here the spin image method is recommended for surfaces with salient global shapes, and the point signature method to match surfaces with many significant local variations.

Furthermore if the measurement surface is a long and narrow patch, the radius of the signature will be relatively very small and not much information is involved in the sphere region of the signature, so that SRS cannot represent the surface shape very well. Fortunately, this rarely occurs in practice.

4. Refinement Based on the Orthogonal Distance Fitting

After initial matching with the structured region signature algorithm, final fitting is performed to optimize the result. The ICP method could be adopted here. Its superiority is that the ICP method can register different types of representations in either continuous or discrete forms. Hence it is not necessarily required to supply a design function or to reconstruct the given discrete template into a continuous function. However, it is very computationally expensive to establish point

correspondances between the two surfaces. False correpondances often appear and it is not easy to distinguish and reject them [37]. Furthermore, the point sets of the given nominal model may be very sparse and consequently the final fitting accuracy is restricted. Therefore this paper adopts a derivative based method and a continuous function is required for the template.

If the measurement data are to be located within a tolerance zone of width t, the orthogonal distances from the measurement points to the associated surface should not be greater than $t/2$ [38, 39]. Thus the refinement result is better when calculated based on the orthogonal distance fitting (ODF); otherwise some points will be overweighted and the fitted results can be biased. NURBS (*Non-Uniform Rational B-Spline*) has become a standard representation in both academy and industry [35] and it is commonly used in CAD models. It is a parametric representation with two foot-point parameters $\{u, v\}$, which are usually normalized into a span $[-1, 1]$. As a result the orthogonal distance matching with parametric templates will be considered,

$$\min_{\mathbf{m}} \sum_{i=1}^{N} \min_{u_i, v_i} \|\mathbf{p}_i - \mathbf{q}_i\|^2 \tag{13}$$

This means, the matching problem is solved in a nested approach. Firstly solve the foot-point parameters $\{u_i, v_i\}$ associated with the orthogonal projection point $\mathbf{q}_i$ on the template for each measurement point $\mathbf{p}_i$ at the inner iteration, and then update the six motion parameters $\mathbf{m} = [\theta_x, \theta_y, \theta_z, t_x, t_y, t_z]^T$ at the outer iteration. A fast and stable method was adopted to calculate projection points on NURBS surfaces [40]. This will not be presented in detail here.

If the reference function is moved into a non-standard position, the representation will become rather complicated. It is proved that moving the measurement data is equivalent to moving the template, and their fitting results are the same [29]. As a consequence transformations are always performed on the measurement data in this paper.

A vector is defined as $\mathbf{g} \in \mathbb{R}^{3N\times 1}$,

$$g_k = \begin{cases} x_i - X_i, & k = 3i-2 \\ y_i - Y_i, & k = 3i-1 \\ z_i - Z_i, & k = 3i \end{cases} , i = 1, 2, \ldots, N$$

where $[X_i, Y_i, Z_i]^T = \mathbf{q}_i$.

Then Equation (13) can be rewritten as,

$$\min_{\mathbf{m}} \sum_{i=1}^{3N} g_k^2 = \min_{\mathbf{m}} \sum_{i=1}^{3N} \mathbf{g}^T\mathbf{g} \tag{14}$$

It can be solved with the Levenberg-Marquardt algorithm [41]

$$\left[\left(\frac{\partial \mathbf{g}}{\partial \mathbf{m}}\right)^T \frac{\partial \mathbf{g}}{\partial \mathbf{m}} + \lambda \mathbf{I}\right] \delta\mathbf{m} = -\left(\frac{\partial \mathbf{g}}{\partial \mathbf{m}}\right)^T \mathbf{m} \tag{15}$$

here $\mathbf{I}$ is a 6×6 identity matrix.

The three rows of the Jacobian matrix $\mathbf{J} = \partial\mathbf{g}/\partial\mathbf{m} \in \mathbb{R}^{3N\times 6}$ associated with the point $\mathbf{p}_i$ are,

$$\begin{bmatrix} \mathbf{J}_{3i-2} \\ \mathbf{J}_{3i-1} \\ \mathbf{J}_{3i} \end{bmatrix} = \frac{\partial \mathbf{p}_i}{\partial \mathbf{m}} - \frac{\partial \mathbf{q}_i}{\partial \mathbf{u}_i}\frac{\partial \mathbf{u}_i}{\partial \mathbf{m}} \tag{16}$$

Here $\mathbf{u}_i = [u_i, v_i]^T$ are the foot-point parameters of $\mathbf{q}_i$. When the measurement point $\mathbf{p}_i$ moves, the closest point $\mathbf{q}_i$ moves as well and the corresponding foot-point parameters $\mathbf{u}_i$ need to be updated simultaneously. Some researchers ignore the parameter dependency for the ease of implementation [32], but the fitting accuracy can be greatly influenced. Here the parameter dependency $\partial\mathbf{u}_i/\partial\mathbf{m}$ will be derived as follows.

Each pair of points are nearest to each other and the following equation always holds true [42],

$$\begin{aligned}
&\frac{\partial}{\partial \mathbf{u}_i}(\mathbf{p}_i - \mathbf{q}_i)^T(\mathbf{p}_i - \mathbf{q}_i) \\
&= -(\frac{\partial \mathbf{q}_i}{\partial \mathbf{u}_i})^T(\mathbf{p}_i - \mathbf{q}_i) \\
&= 0
\end{aligned}$$

For the sake of clarity, the subscript i is omitted and the partial derivatives $\partial\mathbf{q}/\partial\mathbf{u}$ can be rewritten as $\mathbf{q_u}$, so that,

$$\begin{aligned}
&\frac{\partial}{\partial \mathbf{m}}(-\mathbf{q}_\mathbf{u}^T(\mathbf{p} - \mathbf{q})) \\
&= \mathbf{q}_\mathbf{u}^T\mathbf{q}_\mathbf{u}\mathbf{u}_\mathbf{m} - \begin{bmatrix} \mathbf{q}_{uu}^T(\mathbf{p} - \mathbf{q}) & \mathbf{q}_{uv}^T(\mathbf{p} - \mathbf{q}) \\ \mathbf{q}_{uv}^T(\mathbf{p} - \mathbf{q}) & \mathbf{q}_{vv}^T(\mathbf{p} - \mathbf{q}) \end{bmatrix} \mathbf{u}_\mathbf{m} - \mathbf{q}_\mathbf{u}^T\mathbf{p}_\mathbf{m} \\
&= 0
\end{aligned}$$

We obtain,

$$\mathbf{u}_\mathbf{m} = \left\{ \mathbf{q}_\mathbf{u}^T\mathbf{q}_\mathbf{u} - \begin{bmatrix} \mathbf{q}_{uu}^T(\mathbf{p} - \mathbf{q}) & \mathbf{q}_{uv}^T(\mathbf{p} - \mathbf{q}) \\ \mathbf{q}_{uv}^T(\mathbf{p} - \mathbf{q}) & \mathbf{q}_{vv}^T(\mathbf{p} - \mathbf{q}) \end{bmatrix} \right\}^{-1} \mathbf{q}_\mathbf{u}^T\mathbf{p}_\mathbf{m} \tag{17}$$

Substituting Equation (17) into Equation (16), then the increment of the motion parameter vector in Equation (15) can be obtained. λ in Equation (15) is a damping factor used to guarantee convergence and to control the step length at each iteration. If the matrix $\mathbf{A} = \mathbf{J}^T\mathbf{J}$ is not positive-definite, or it is ill-conditioned, the solution will be very unstable or even become divergent. Since $\mathbf{A}$ is a positive-semidefinite Hermitian matrix, according to the spectral theorem,the singular values are the same with its eigen-values [43], i.e.

$$\mathbf{A} = \mathbf{U}\mathbf{S}\mathbf{U}^T$$

where $\mathbf{U} \in \mathbb{R}^{6\times6}$ is an orthogonal matrix and $\mathbf{S} = diag\{\sigma_1, \sigma_2, \ldots, \sigma_6\}$. Here $\sigma_1 \geq \sigma_2 \geq \ldots \geq \sigma_6$ are the singular values. It is evident that,

$$\mathbf{A} + \lambda\mathbf{I} = \mathbf{U}(\mathbf{S} + \lambda\mathbf{I})\mathbf{U}^T$$

Therefore the singular value decomposition does not need to be performed twice and the new singular values are $\{\sigma_i' | \sigma_i' = \sigma_i + \lambda, i = 1, 2, \ldots, 6\}$. A very large λ will reduce the step length of the motion parameters and a very small singular value will make the solution unstable [44]. Consequently λ is selected according to the value of σ_6. If $\sigma_6 > \epsilon$, where ϵ is a user-set threshold, e.g. 10^{-7}, then $\lambda = 0$; otherwise set $\lambda = \epsilon - \sigma_6$.

5. Numerical Experiments

In the present paper all the programmes were coded with MATLAB 7 and run on a 3GHz Pentium 4 PC, with 2GB of RAM.

The *peaks* function is commonly utilized in numerical computation [45]. It was adopted to represent the shape of the reference template and modelled with NURBS. A small section was chosen from the template as the measured surface and moved to an arbitrary position as a situation before matching, as shown in Figure 3

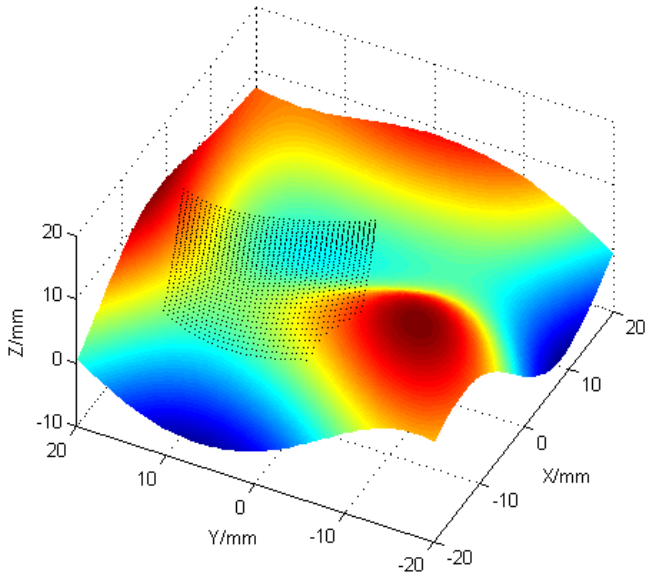

Figure 3. The relative position before matching

The data points were sampled with a spacing $d = 0.5$mm, which is a normal scanning density of coordinate measuring machines. *The Fractional Brownian Motion* illustrated in Figure 4 [46] was employed to simulate noise. Noise with mean value 0 and standard deviation 0.5μm was added to the x, y and z coordinates of the data points respectively.

The nominal points were sampled uniformly with a spacing $d = 0.5$ mm as well. The rough matching was performed with SRS. As the surface is very smooth, the signature centres were uniformly sampled on the template surface. If the spacing between these centres was adopted to be $D = R/3$ ($R = 9.813$mm is the radius of the signature sphere) and N_c =50 data points were sampled on each signature curve, the matching result is shown in Figure 5(a).

Then the orthogonal distance fitting was undertaken onto the rough-matched data and template. In order to speed up point projection the whole NURBS template was divided into Bézier patches and then the foot-point parameters of the projection points were solved using the Newton-Raphson algorithm [40]. Three outer iterations were implemented to update the six motion parameters. To evaluate the quality of the refinement result, the relative angular and translational errors of the fitted result with respect to the ideal location are given in Table 1. Since the optimization was implemented by minimising the sum of squared orthogonal distances, the residual

is also represented using the orthogonal distances. However, the data points are sampled uniformly on the X–Y plane, instead of on the surface, thus the sampling space has been changed and the height parameters S_a and S_q [47] cannot be obtained by simply calculating the mean values, and resampling is required. Here the peak-to-valley parameter P–V is adopted to evaluate the amplitude of the residuals. For consistency, the orthogonal distances associated with the rough-matched data by SRS are also calculated, although SRS does not need to calculate these distances or even a continuous representation is not required for the template. The corresponding S_z parameter is also presented in Table 1.

Table 1. The matching result of the two-stage strategy

Method	Angular error (°)			Positional error(mm)			P–V (μm)	Time(sec)
	θ_x	θ_y	θ_z	t_x	t_y	t_z		
SRS	0.91	0.83	1.75	0.18	0.27	-0.11	601	0.40
ODF	-1.06e-3	-3.81e-4	-3.08e-3	-2.13e-5	6.54e-4	-5.24e-5	5.30	6.270

From this table we can see that SRS can find a very good rough match. Theoretically the translational error of SRS is no greater than D and the rotational error of the azimuth angle ϕ is no greater than $2\pi/N_c$.

Table 1 shows ODF improves the matching accuracy by three orders and the residual achieves the same amplitude as the introduced noise, i.e. an accurate matching is established and the relative form deviation of the measured data with respect to the nominal shape can be evaluated accordingly.

To demonstrate the superiority of the procedure presented in this paper, it was compared with the most commonly used registration technique ICP (Iterative Closest Point). The correspondance relationship between point pairs is established using the k-D tree [48] and the motion parameters are worked out with the singular value decomposition technique [49]. Both ODF and ICP are run 25 iterations and their rotational and translational errors at each iteration are listed in Figures 6(a) and 6(b) respectively.

The ODF result converges after only three iterations. Its convergence rate depends on the relative value of the residual, i.e. on the quality of rough matching and the amplitude of noise. If the SRS matching result is good enough, the convergence rate can achieve a quadratic order, as shown in this example. Otherwise the motion parameters will converge linearly. In some cases when the rough position is beyond the convergence domain of ODF, the fitting result may be incorrect or even diverge[50]. However, the convergence rate of ICP is linear, and usually ICP needs more than 20 iterations to obtain a good matching between two point sets. Moreover, it tends to be trapped at a local minimum. Especially when both the template and data points have nearly the same density and the same distribution mode, ICP will intend to overlap point pairs, instead of finding the best matching between the two surfaces [51], i.e. it is the lateral point locations, instead of the geometrical shapes of the surfaces that determine the matching result. That is why ICP cannot overcome the relative shift in the y direction (approximately $d/2$) in Figure 6(b).

Therefore ICP is not preferable for the applications in precision metrology, and the derivative-based methods which employ continuous template functions always deserve a prior consideration. If the representation of the reference surface is very complicated, which causes the derivatives very difficult to be obtained, the finite difference method

can be utilized[52].

6. Conclusions and Future Work

To assess the form quality of a freeform surface, the measured data need to be matched with the reference template. In this paper the whole matching procedure is divided into two stages, initial matching and final matching.

An initial matching algorithm called the Structured Region Signature is proposed. It represents the surface shape with a one-dimensional signature profile, thus is very efficient and straightforward to implement. The signature is a global feature of a surface, and not sensitive to measurement noise and local surface variation. The accuracy of rotation is determined by the sampling density of points on each signature profile, whereas the accuracy of translation is restricted by the sampling spacing of the candidate signature centres on the template.

When an approximate position is supplied, the final optimization is performed thereafter. It is carried out by minimising the sum of squared orthogonal distances from the measured data to the reference surface. It is consistent with the definition of form deviations in ISO standards and the bias in the fitted parameters can be greatly reduced. Compared with the extensively used ICP method, it shows superiority in both accuracy and efficiency. The least squared distances adopted here is the best estimator when the noise in the data obeys the normal distribution. But in practice the distribution of errors may be in other forms and the data probably include defects or outliers, which may cause significant error in the matching result. Hence the objective function of refinement will be adopted according to the distribution of the measurement errors. Various robust estimators such as the ℓ_1 norm [53], the least median deviation [54], the reweighted least squares [55] et al will be investigated to improve the robustness and accuracy of the final matching programme.

Acknowledgements

The authors gratefully acknowledge the Royal Society for a Wolfson Research Merit Award and the European Research Council for its programme ERC-2008-AdG 228117-Surfund.

References

[1] Goch G, Tschudi U 1992 A universal algorithm for the alignment of sculptured surfaces *Annals of the CIRP* **41** 597-600.
[2] ISO/TS 17450-1:2005 *Geometrical Product Specifications (GPS)-General Concepts-Part 1: Model for Geometrical Specification and Verification.*
[3] Hume K J 1970 *Engineering Metrology* 3rd Ed, MacDonald Technical & Scientific, London.
[4] Jastram M O 1996 *Inspection and Feature Extraction of Marine Propellers*, MSc Thesis, MIT, USA.
[5] Malacara D 2007 *Optical Shop Testing* 3rd Ed, John Wiley&Sons
[6] Li Y, Gu P 2005 Inspection of free-form shaped parts *Robotics and Computer-Integrated Manufacturing* **21**(4-5) 421-430.
[7] Wang P J, Chen J H, Li Z Q et al 1997 A new algorithm for the profile error of a parameter surface *J Huazhong Univ. Sci. and Technol.* **25**(3)1-4.
[8] Cheung C F, Li H F, Kong L B et al 2006 Measuring ultra-precision freeform surfaces using a robust form characterization method *Meas. Sci. Technol.* **17** 488-494.
[9] Kyprianou L 1980 *Shape Classification in Computer-Aided Design* PhD Thesis, Cambridge University, UK.

[10] Joshi S, Chang T C 1988 Graph-based heuristics for recognition of matching features from a 3D solid model *Computer Aided Design* **20**(2) 58-66.
[11] Brown L G 1992 A survey of image registration techniques *ACM Computing Surveys* **24**(4) 325-376.
[12] Groemer H 1996 *Geometric Applications of Fourier Series and Spherical Harmonics*, Cambridge University Press.
[13] Zhang C, Chen T 2001 Efficient feature extraction for 2D/3D objects in mesh representation *IEEE Int. Conf. Image Proc* Thessakoniki, Greece.
[14] Sukumar S R 2004 *Curvature Variation as Measure of Shape Information* Master Thesis, University of Tennessee, USA.
[15] Gelfand N, Mitra N J, Guibas L J et al 2005 Robust global registration. In Desbrun M,Pottmann H, Editors *Eurographics Symp. on Geometry Proc.* 197-205.
[16] Iyer N, Jayanti S, Lou K et al 2005 Three-dimensional shape searching: state-of-the art review and future trends *Computer Aided Design* **37** 509-530.
[17] Planitz B M, Maeder A J, Williams J A 2005 The correspondence framework for 3D surface matching algorithms *Computer Vision and Image Understanding* **97** 347-383.
[18] Johnson A E 1997 *Spin-Images: a Representation for 3-D Surface Matching* PhD Thesis,Carnegie Mellon University, USA.
[19] Chua C, Jarvis R 1997 Point signatures: a new representation for 3D object recognition *Inter. J. Comput. Vision* **25** (1) 63-85.
[20] Ashbrook A, Fisher R, Werghi N, Robertson C 1998 Aligning arbitrary surfaces using pairwise geometric histograms *Proc. Noblesse Workshop on Non-linear Model Based Image Analysis*, Glasgow, Scotland 103-108.
[21] Horn B K P 1987 Closed-form solution of absolute orientation using unit quaternions *J Opt. Soc. Am.* **4**(4)629-642.
[22] Besl P J, McKay N D 1992 A method for registration of 3-D shapes *Trans. Patt. Anal. and Machine Intell.* **14**(2)239-256.
[23] Krsek P, Pajdla T, Hlavác V 2002 Differential invariants as the base of triangulated surface registration *Computer Vision and Image Understanding* **87**(1-3) 27-38.
[24] Rusinkiewicz S, Levoy M 2001 Effiient variants of the ICP algorithm *3rd Inter. Conf. 3D Digital Imaging and Modeling* 145-152.
[25] Press W H, Teukolsky S A, Vetterling W T 2002 *Nnumerical Recipes in C++* 2nd ed, Cambridge University Press.
[26] Forbes A B 1990 Least squares best fit geometric elements *Algor for Approx II* ed J C Mason and M G Cox. 311-319 (London: Chapman and Hall)
[27] Zhang Z 1997 Parameter estimation techniques: a tutorial with application to conic fitting *Image and Vision Computing 15*(1) 59-79.
[28] Ahn S J, Rauh W, Warnecke H J 2001 Least-squares orthogonal distances fitting of circle sphere, ellipse, hyperbola and parabola *Patt. Recog.* **34**(12) 2283-2303.
[29] Atieg A, Watson G A 2003 A class of methods for fitting a curve or surface to data by minimizing the sum of squares of orthogonal distances *J Computat. and Appl. Math* **158**(2) 277-296.
[30] Fitzgibbon A W 2003 Robust registration of 2D and 3D point sets *Image and Vision Computing* **21** 1145-1153
[31] Boggs P T, Byrd R H, Schnabel R B 1987 A stable and efficient algorithm for nonlinear orthogonal distance regression *SIAM J Stat Comput* **8**(6) 1052-1078.
[32] Sourlier D M 1995 *Three Dimensional Feature Independent Bestfit in Coordinate Metrology*, PhD Thesis, Swiss Federal Inst. of Technol. Zürich.
[33] Hoppe H, DeRose T, Duchamp T et al 1992 Surface reconstruction from unorganized points *Comput. Graphics* **26**(2) 71-78.
[34] Barker R M, Cox M G, Forbes A B et al 2004 *Discrete Modelling and Experimental Data Analysis* NPL Report
[35] Piegl L, Tiller W 1997 *The NURBS Book* 2nd ed, Springer-Verlag, New York.
[36] Grimson W E L,Lozano-Perez T 1984 Model-based recognition and localization from sparse range or tactile data *Inter. J. Robotics Res.* **3**(3) 3-35.
[37] Xiao G, Ong S H, Foong K W C 2006 Registration of partially overlapping surfaces by rejection of false point correspondences *Patt. Recog.* **39** 373-383.
[38] DIN 32880-1:1986 *Coordiante Metrology-Geometrical Fundamental Principles, Terms and Definitions*, German Standard, Beuth Verlag, Berlin.
[39] ISO 1101:2004 *Geometrical Product Specifications (GPS)-Geometrical Tolerancing-Tolerances of Form, Orientation, Locatoin and Run-out.*
[40] Zhang X, Jiang X, Scott P J et al 2009 A fast point projection approach of NURBS surfaces

Algor. for Approx. VI ed J Levesley et al (Springer)
[41] Marquardt D W 1963 An algorithm for least squares estimation of nonlinear parameters *J. Soc. Indust. Appl. Math.* **11**(2) 431-441.
[42] Ahn S J 2004 *Least Squares Orthogonal Distance Fitting of Curves and Surfaces in Space*, Springer.
[43] Halmos P 1963 What does the spectral theorem say? *Am. Math. Monthly* **70**(3)241-247.
[44] Hansen P C 1998 *Rank-Deficient and Discrete Ill-Posed Problems*, SIAM.
[45] *MATLAB 7 Function Reference:Volume 3 (P-Z)*, MATLAB help documentation, MathWorks, USA, 2009
[46] Mandelbrot B B, Van Ness J W 1968 Fractional Brownian motions, fractional noises and applications *SIAM Review* **10** 422-437.
[47] ISO/DIS 25178-2:2007 *Geometrical product specifications (GPS) - Surface texture: Areal - Part 2: Terms, definitions and surface texture parameters*
[48] Bentley J L 1990 K-D trees for semidynamic point sets *Proc. 6th Annual Symp Comput Geom.*187-197.
[49] Eggert D W, Lorusso A, Fisher R B 1997 Estimating 3-D rigid body transformations: a comparison of four major algorithms *Mach. Vis. and Appl.* **9**(5-6)272-290
[50] Pottmann H, Huang Q X, Yang Y L et al 2006 Geometry and convergence analysis of algorithms for registration of 3D shapes *Int. J. Computer Vision* **67**(3)277-296
[51] Zhang X 2009 *Free-Form Surface Fitting for Precision Coordinate Metrology*, PhD Thesis. University of Huddersfield, UK
[52] Morton K W, Mayers D F 2005 *Numerical Solution of Partial Differential Equations, An Introduction*, Cambridge University
[53] Watson G A 2000 Some robust methods for fitting parametrically defined curves or surfaces to measured data *Adv. Math. and Comput. Tools in Metrology IV*, World Scientific, Singapore 256-272.
[54] Rousseeuw P J, Leroy A M 1987 *Robust Regression and Outlier Detection*, John Wiley & Sons, New York.
[55] Holland P W, Welsch R E 1977 Robust regression using iteratively reweighted least-squares *Communications in Statistics: Theory and Methods* **6**(9)813-827.

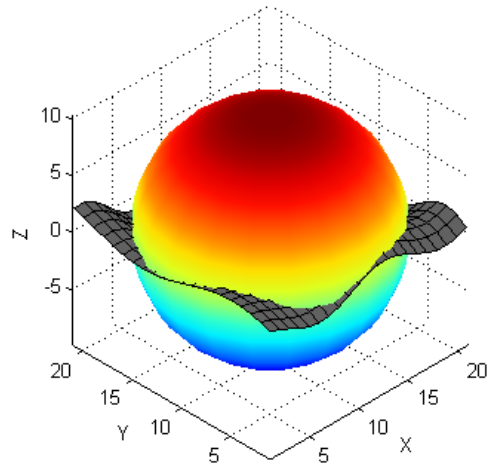
Z
10
5
0
-5
20
15
Y
10
5
5
10
15
20
X

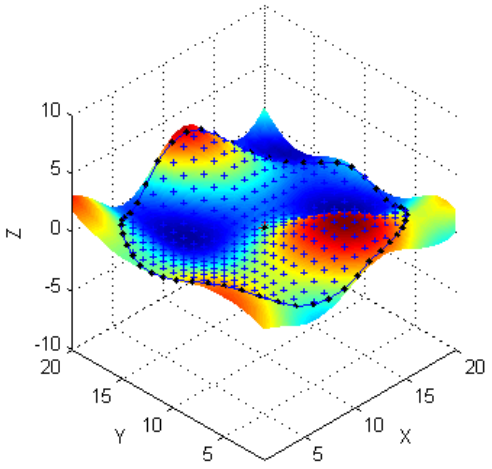
Z
10
5
0
-5
-10
20
15
Y
10
5
5
10
15
20
X

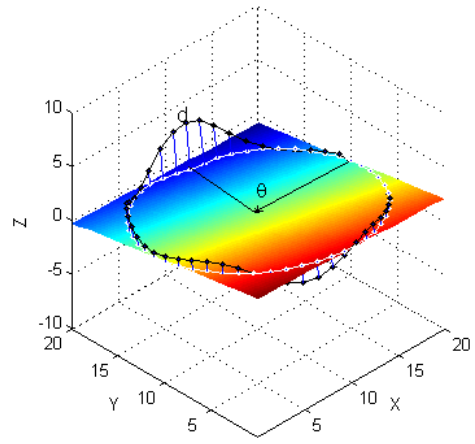
d
θ
Z
10
5
0
-5
-10
20
15
Y
10
5
5
10
15
20
X

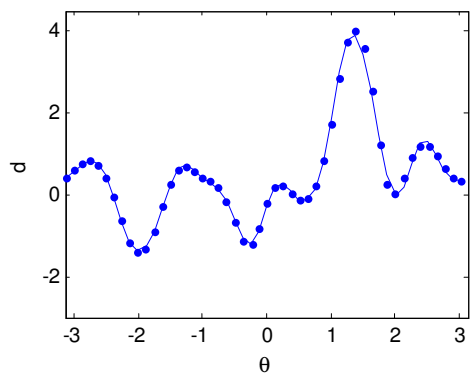
d
4
2
0
-2
-3
-2
-1
0
1
2
3
θ

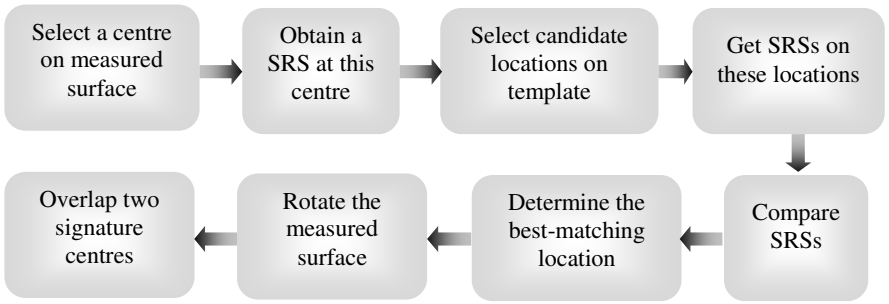

Figure 2. Procedure of SRS matching

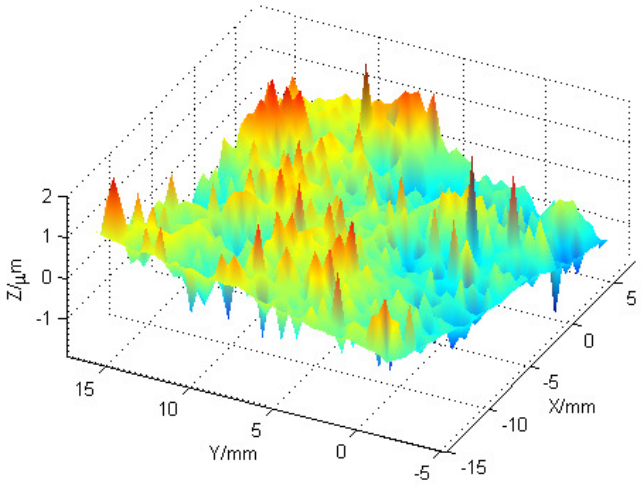

Figure 4. Noise simulated with the fractional Brownian motion

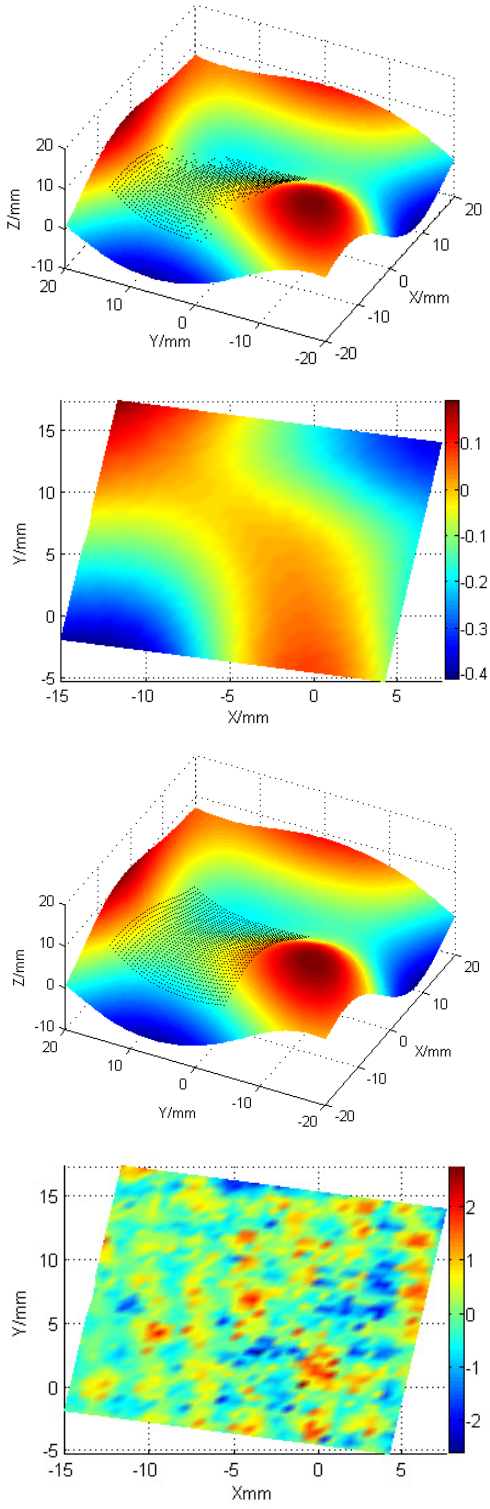

Figure 5. Matching results and residuals: (a)SRS result, (b)SRS residual(mm), (c)ODF result and (d)ODF residual(μm)

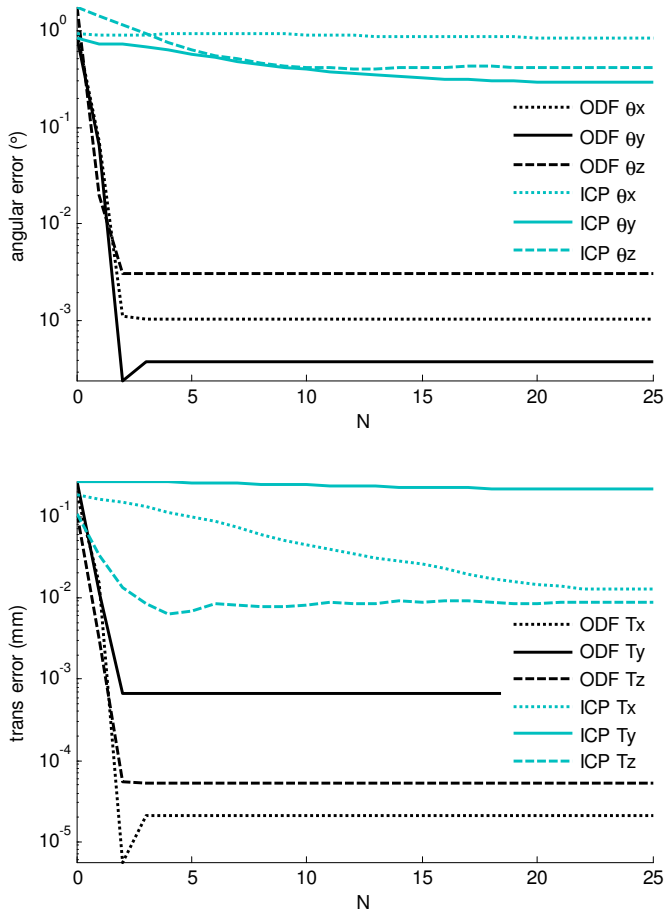

Figure 6. Comparison of two refinement methods:(a)Angular error and (b)Translational error